Letter

Charge noise suppression in capacitively coupled singlet-triplet spin qubits under magnetic field

Guo Xuan Chan [1,2] J. P. Kestner,[3] and Xin Wang [1,2,*]

[1]*Department of Physics, City University of Hong Kong, Tat Chee Avenue, Kowloon, Hong Kong SAR, China*

[2]*City University of Hong Kong Shenzhen Research Institute, Shenzhen, Guangdong 518057, China*

[3]*Department of Physics, University of Maryland Baltimore County, Baltimore, Maryland 21250, USA*

(Received 19 November 2020; revised 3 March 2021; accepted 16 April 2021; published 27 April 2021)

Charge noise is the main hurdle preventing high-fidelity operation, in particular that of two-qubit gates, of semiconductor-quantum-dot-based spin qubits. While certain sweet spots where charge noise is substantially suppressed have been demonstrated in several types of spin qubits, the existence of one for coupled singlet-triplet qubits is unclear. We theoretically demonstrate, using full configuration-interaction calculations, that a range of nearly sweet spots appears in the coupled singlet-triplet qubit system when a strong enough magnetic field is applied externally. We further demonstrate that ramping to and from the judiciously chosen nearly sweet spot using sequences based on the shortcut to adiabaticity offers maximal gate fidelities under charge noise and phonon-induced decoherence. These results should facilitate realization of high-fidelity two-qubit gates in singlet-triplet qubit systems.

DOI: 10.1103/PhysRevB.103.L161409

I. INTRODUCTION

Singlet-triplet qubits, defined by two-electron spin states confined in semiconductor double-quantum-dot (DQD) devices, are promising candidates for the realization of large-scale quantum-dot quantum computation [1–12]. In these systems, the charge noise directly affects the control over the spin qubits and is thus the key obstacle preventing high-fidelity quantum control [13–19]. A useful strategy to mitigate charge noise is to operate the qubits near the so-called sweet spots where the control (e.g., the exchange interaction between spins) is first order insensitive to charge noise [20–32]. While this strategy has been successfully demonstrated in a variety of single-qubit devices, the existence of any sweet spot, in particular for two singlet-triplet qubits, is far less obvious.

Entangling operations between singlet-triplet qubits are typically carried out by exploiting either the capacitive interaction [2,33–43] or exchange coupling [44–50] between two DQD devices. Capacitive gates are achieved when the tunneling between the two DQDs is suppressed, while the Coulomb interaction mediates the interqubit interaction. Exchange gates, on the other hand, are mediated by the exchange coupling between two neighboring spins between two DQDs, which can be manipulated by interdot tunneling and energy detuning between the two spins. In this work, we focus on capacitively coupled singlet-triplet qubits.

Gate operations on two singlet-triplet qubits coupled by capacitive interactions typically have fidelities of ∼72% [2] and can be improved to ∼90% [34] by applying a large magnetic gradient. However, to meet the stringent requirement for quantum error correction, suppression of charge noise becomes emergent. Theoretical calculations [33], particularly using variations of the configuration interaction (CI) method [41–44], are widely employed to search for the sweet spots. Reference [42] proposed that there exists a sweet spot when the two singlet-triplet qubits are aligned at an appropriate angle, while Ref. [40] claims that a sweet spot may appear at a certain detuning value. However, these results are obtained from the Hund-Mulliken approximation keeping the lowest orbital in each quantum dot, and it is unclear whether the results hold when higher orbitals are taken into account. Furthermore, Ref. [40] assumed that the charge states of each qubit are independent of each other, but that assumption breaks down in the parameter regime where the sweet spot was claimed to occur. References [35–37], using a more sophisticated CI method either by involving excited orbitals or by populating the quantum-dot system with *s*-type Gaussian functions, showed that, while a sweet spot may exist for the capacitive two-qubit coupling, it is *not* at the same time a sweet spot for single-qubit exchange interactions, which limits the usefulness of those prior results in experiments.

All these previous CI calculations were performed without an external magnetic field. In this Letter, we show, using full CI calculations, that a range of *nearly* sweet spots appear in the coupled singlet-triplet qubit system, when a strong enough magnetic field is applied externally. Around these nearly sweet spots, both the capacitive coupling and the single-qubit exchange interactions are very weakly dependent on the charge noise, making possible high-fidelity manipulations. We demonstrate that operating in the nearly-sweet-spot regime yields the entangling gate with a fidelity much higher than in the previous proposals [34,35]. Moreover, the extended range of this nearly-sweet-spot regime allows for application of shortcuts to adiabaticity for the ramping pulses to and from the operating point, which leads to about one order of magnitude improvement in the gate fidelity. In contrast to [34] in which

*x.wang@cityu.edu.hk

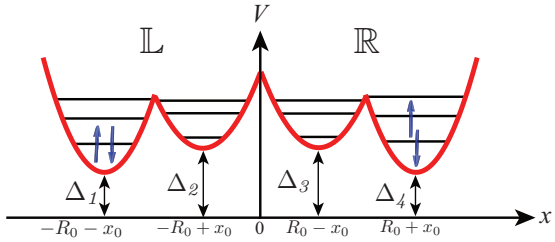

FIG. 1. Schematic illustration of the model potential given in Eq. (1).

the high-fidelity entangling gate results from application of a large magnetic gradient on singly occupied dots, our model benefits from strong capacitive coupling with weak coupling to charge noise. Our results should facilitate realization of high-fidelity two-qubit gates in singlet-triplet qubit systems.

II. MODEL

We consider an n-electron system $H = \sum h_j + \sum e^2/\epsilon|\mathbf{r}_j - \mathbf{r}_k|$ with the single-particle Hamiltonian $h_j = (-i\hbar\nabla_j + e\mathbf{A}/c)^2/2m^* + V(\mathbf{r}) + g^*\mu_B\mathbf{B}\cdot\mathbf{S}$. The confinement potential of a double double-quantum-dot (DDQD) device can be modeled in the xy plane as (see Fig. 1)

$$V(\mathbf{r}) = \tfrac{1}{2}m^*\omega_0^2 \mathrm{Min}[(\mathbf{r}-\mathbf{R}_1)^2 + \Delta_1, (\mathbf{r}-\mathbf{R}_2)^2 + \Delta_2, (\mathbf{r}-\mathbf{R}_3)^2 + \Delta_3, (\mathbf{r}-\mathbf{R}_4)^2 + \Delta_4], \quad (1)$$

where $\mathbf{R}_j = (\pm R_0 \pm x_0, 0)$ are the minima of the parabolic wells [51]. The interdot distance is $2x_0$, while the inter-DQD distance is $2R_0$.

With each DQD hosting one singlet-triplet qubit, the DDQD defines a pair of capacitively coupled singlet-triplet qubits. The two-qubit logical states are $|SS\rangle$, $|ST\rangle$, $|TS\rangle$, and $|TT\rangle$, where $|S\rangle$ and $|T\rangle$ are spin-singlet and unpolarized spin-triplet ($S_z = 0$) states, respectively. Without a magnetic field gradient, the system Hamiltonian H_{int} is diagonal in the bases of logical states as [38–41]

$$H_{\mathrm{int}} = J_{\mathbb{L}}^{\mathrm{eff}}\sigma_z \otimes I + J_{\mathbb{R}}^{\mathrm{eff}} I \otimes \sigma_z + \alpha\sigma_z \otimes \sigma_z, \quad (2)$$

where

$$\alpha = \tfrac{1}{4}(E_{|SS\rangle} - E_{|ST\rangle} - E_{|TS\rangle} + E_{|TT\rangle}), \quad (3a)$$

$$J_{\mathbb{L}}^{\mathrm{eff}} = \tfrac{1}{4}[E_{|TT\rangle} - E_{|SS\rangle} - (E_{|ST\rangle} - E_{|TS\rangle})], \quad (3b)$$

$$J_{\mathbb{R}}^{\mathrm{eff}} = \tfrac{1}{4}[E_{|TT\rangle} - E_{|SS\rangle} + (E_{|ST\rangle} - E_{|TS\rangle})]. \quad (3c)$$

The effective exchange energies $J_{\mathbb{L}}^{\mathrm{eff}}$ and $J_{\mathbb{R}}^{\mathrm{eff}}$ for the qubit defined in the left ($\mathbb{L}$) and right ($\mathbb{R}$) DQDs, respectively, contain both the individual exchange energy of the DQD in the absence of the other, as well as a capacitive shift caused by the neighboring DQD. α is the capacitive interqubit coupling.

We solve the problem using the full configuration interaction (FCI) technique [52], detailed in Sec. I of the Supplemental Material [53]. We use parameters appropriate for GaAs, where the permittivity $\epsilon = 13.1\epsilon_0$, effective electron mass $m^* = 0.067m_e$, confinement strength of the quantum dots $\hbar\omega_0 = 1$ meV, effective Bohr radius $a_B = \sqrt{\hbar/m^*\omega_0} \approx 34$ nm, $x_0 = 2.5a_B$, and $R_0 = 9a_B$. The interqubit distance R_0 is chosen such that the tunneling between

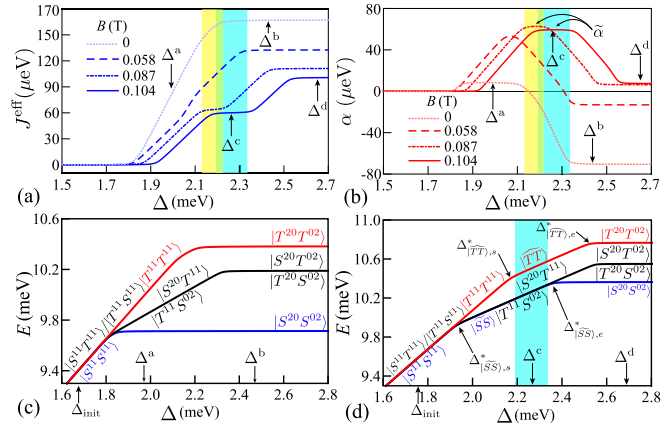

FIG. 2. Nearly sweet spots in the outer detuning scheme. (a) and (b) J^{eff} and α vs detuning Δ for several magnetic field strengths B as indicated. (c) and (d) Energy levels vs detuning Δ for (c) $B = 0$ and (d) $B = 0.104$ T. $\Delta^{\mathrm{a,b,c,d}}$ (Δ_{init}) are proposed operating (initialization) points which will be discussed later. The yellow and cyan areas indicate the nearly-sweet-spot regime for $B = 0.087$ and 0.104 T, respectively, and their overlap, indicated by the green area, should be considered as belonging to both. Note that $|\widetilde{SS}\rangle$ and $|\widetilde{TT}\rangle$ exist for a very small range in (c) and are therefore not indicated (see Sec. IV in [53] for more details).

qubits is negligible; thus, only the capacitive coupling remains. The parameters are summarized in Sec. II in the Supplemental Material. Practically, we truncate the FCI calculation using a cutoff scheme [52], keeping orbitals up to $n = 4$ Fock-Darwin states.

III. RESULTS

A. Nearly sweet spot

We consider only symmetric detuning of two qubits; that is, the detuning values on both qubits are equal. There are thus three possibilities:

$$\begin{aligned}\text{Outer: } &\Delta_2 = \Delta_3 = \Delta > 0, \Delta_1 = \Delta_4 = 0,\\ \text{Center: } &\Delta_1 = \Delta_4 = \Delta > 0, \Delta_2 = \Delta_3 = 0,\\ \text{Right: } &\Delta_1 = \Delta_3 = \Delta > 0, \Delta_2 = \Delta_4 = 0. \end{aligned} \quad (4)$$

In the main text, we focus on the outer scheme where $J_{\mathbb{L}}^{\mathrm{eff}} = J_{\mathbb{R}}^{\mathrm{eff}} \equiv J^{\mathrm{eff}}$, and a discussion on the others can be found in Sec. V of the Supplemental Material [53].

Figures 2(a) and 2(b) show the dependence of J^{eff} and α on detuning Δ under different magnetic fields, which is the key result of this paper. When $B = 0$, α develops two flat regimes. A sweet spot exists for α around $\Delta \approx 2$ meV, but the same Δ range does not give any nearly sweet spots in J^{eff}. This result is consistent with Refs. [2,35–37]. Another regime where both J^{eff} and α have nearly sweet spots is for $\Delta \gtrsim 2.3$ meV. This was envisaged by [54] based on single DQD results in the far-detuned regime, but ramping to such high detuning would expose the qubit to severe leakage or decoherence, which is therefore impractical. Increasing B moves the sweet spot for α at $\Delta \approx 2$ meV to the right, while a nearly-sweet-spot regime gradually appears for J^{eff} at $B \gtrsim 0.087$ T. At $B = 0.104$ T, the nearly-sweet-spot regime where both J^{eff} and α are very

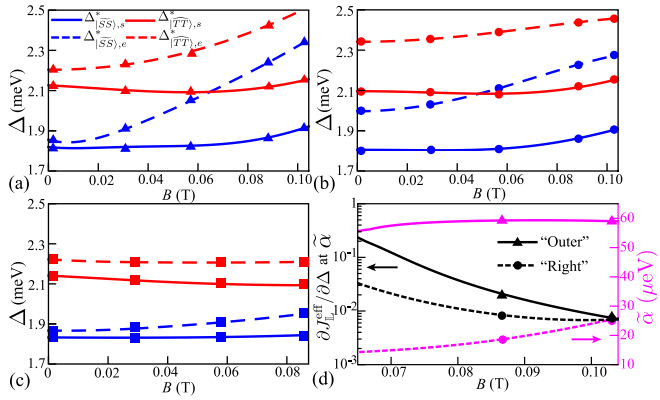

FIG. 3. $\Delta^*_{|\widetilde{SS}\rangle,s}$, $\Delta^*_{|\widetilde{SS}\rangle,e}$, $\Delta^*_{|\widehat{TT}\rangle,s}$, and $\Delta^*_{|\widehat{TT}\rangle,e}$ as a function of magnetic field strength B in the (a) outer, (b) right, and (c) center detuning schemes. (d) Black curves (using the left y axis): the values of $\partial J^{\rm eff}_{\mathbb{L}}/\partial\Delta$ evaluated at the Δ value where α reaches its maximal value $\widetilde{\alpha}$. Magenta curves (using the right y axis): the maximal values of α (i.e., $\widetilde{\alpha}$) vs the magnetic field. The symbols in magenta and black represent results from the same detuning scheme.

weakly dependent on Δ is quite extended, as indicated by the cyan area. At the same time, the α value is enhanced to reduce the gate time and minimize the accumulation of gate error. We shall see later that the detuning $\Delta^{\rm c}$ yields the highest gate fidelity. We also note that when α reaches its maximal value $\widetilde{\alpha}$, $\partial\alpha/\partial\Delta = 0$, while at the same Δ value $\partial J^{\rm eff}/\partial\Delta$ is small ($\sim 10^{-2}$) but not exactly zero [see Fig. 3(d)]. This is the reason we call the region *nearly* sweet spots. It is also found that the nearly-sweet-spot region exists for asymmetric cases, e.g., the elliptical confinement potential or asymmetric confinement strengths, where the details are referred to Secs. XIII and XV in the Supplemental Material, respectively.

Figures 2(c) and 2(d) show the energy level structure of the system as the detuning is varied. The states are labeled using a Dirac ket with the first entry being the state of the left DQD and the second being the right DQD. The state of one qubit (i.e., one DQD) is either a singlet (S) or a triplet (T), with the superscript showing the charge configurations. For example, the four-electron state shown in Fig. 1 can be understood as $|S^{20}T^{02}\rangle$ [55]. Detailed discussions of all relevant states in terms of the extended Hubbard model can be found in Sec. IV of the Supplemental Material [53].

Figure 2(c) shows the energy levels at zero magnetic field. All levels are parallel for $\Delta \gtrsim 2.3$ meV, consistent with the observation that both $J^{\rm eff}$ and α are weakly dependent on Δ in this range. Around $\Delta \approx 2$ meV, the slopes of the curves can be combined in the fashion of Eq. (3a), implying that $\partial\alpha/\partial\Delta \approx 0$, but not for $J^{\rm eff}$ [Eqs. (3b) and (3c)], consistent with the observations from Figs. 2(a) and 2(b). When a magnetic field $B = 0.104$ T is applied, however, the situation changes. Two new states become significant: a bonding state $|\widetilde{SS}\rangle = (|S^{11}S^{02}\rangle + |S^{20}S^{11}\rangle)/\sqrt{2}$ and an antibonding state $|\widehat{TT}\rangle = (|T^{11}T^{02}\rangle - |T^{20}T^{11}\rangle)/\sqrt{2}$ [55]. These two states cover an extended Δ range in the energy levels. We can find the starting (s) and ending (e) points of these ranges by setting equal the energies of the states admixed at the avoided crossing points. For example, the starting point $\Delta^*_{|\widetilde{SS}\rangle,s}$ is found by setting the energies of $|\widetilde{SS}\rangle$ and $|S^{11}S^{11}\rangle$ equal, while the ending point $\Delta^*_{|\widehat{TT}\rangle,e}$ is found by setting the energies of $|\widehat{TT}\rangle$ and $|T^{20}T^{02}\rangle$ equal. It is interesting to note that there exists a Δ range (the cyan area) where levels $|\widehat{TT}\rangle$, $|\widetilde{SS}\rangle$, $|S^{20}T^{11}\rangle$, and $|T^{11}S^{02}\rangle$ share *almost* the same slope with respect to Δ ($\approx$0.996), making the Δ derivatives of the right-hand side of Eqs. (3a)–(3c) almost vanish altogether. This is the origin of the nearly-sweet-spot range for both $J^{\rm eff}$ and α. The existence of this range is actually not specific to the parameters chosen here. A discussion of the generality of its existence is presented in Sec. VI of the Supplemental Material [53].

The relevant lowest-energy levels of the DDQD system can be interpreted well using the extended Hubbard model [53], allowing us to interpolate the FCI results to cover a range of parameters. Figures 3(a)–3(c) show the values of $\Delta^*_{|\widetilde{SS}\rangle,s}$, $\Delta^*_{|\widetilde{SS}\rangle,e}$, $\Delta^*_{|\widehat{TT}\rangle,s}$, and $\Delta^*_{|\widehat{TT}\rangle,e}$ as functions of magnetic field in the outer, right, and center detuning schemes, respectively. The symbols are data points extracted from the FCI calculation, and the lines are interpolations using the extended Hubbard model. We see that only the outer and right detuning schemes give $\Delta^*_{|\widetilde{SS}\rangle,e} > \Delta^*_{|\widehat{TT}\rangle,s}$ for sufficiently strong magnetic field, implying an overlapping region of $|\widetilde{SS}\rangle$ and $|\widehat{TT}\rangle$. No overlap occurs for the center detuning scheme as $\Delta^*_{|\widetilde{SS}\rangle,e}$ is less sensitive to magnetic field. In addition, the Δ range of the overlap for the outer scheme increases roughly linearly with the magnetic field for the values concerned, while there is a moderate increase for the right scheme, resulting in $\approx$0.2 meV for the former and $\approx$0.1 meV for the latter at $B = 0.104$ T. Figure 3(d) shows the maximal value of α, $\widetilde{\alpha}$, in the nearly-sweet-spot regime, as well as $\partial J^{\rm eff}_{\mathbb{L}}/\partial\Delta$ evaluated at the same Δ value where α reaches maximum ($\partial\alpha/\partial\Delta = 0$), for the outer and right schemes. For both schemes, $\partial J^{\rm eff}_{\mathbb{L}}/\partial\Delta$ is as small as $\sim 10^{-2}$ for $B \gtrsim 0.1$ T, indicating that the susceptibility to charge noise is extremely weak. On the other hand, $\widetilde{\alpha}$ is much greater for the outer scheme than the right one, suggesting that the outer scheme remains the optimal protocol to operate the coupled DDQD systems.

B. CPHASE gate

The interqubit coupling $\sigma_z \otimes \sigma_z$ gives rise to a controlled-phase (CPHASE) gate [35,36]. The system is initialized at $\Delta_{\rm init}$ where α is negligible and is then ramped to a larger detuning, $\Delta_{\rm op}$, where the operation is performed with a reasonably strong α. This ramping time is denoted as $\tau_{\rm ramp}$. After operating at $\Delta_{\rm op}$ for a time $\tau_{\rm op}$, the system is brought back to $\Delta_{\rm init}$ in $\tau_{\rm ramp}$ [see Fig. 4(a)]. The total gate time is therefore $\tau = 2\tau_{\rm ramp} + \tau_{\rm op}$.

The evolution of the system in the logical subspace can be described by the master equation,

$$\begin{aligned}\dot{\rho} = &-i[H_{\rm int},\rho] + \left(\gamma_{\varphi_{\mathbb{L}}} + \gamma_{{\rm dep}_{\mathbb{L}}}\right)\mathcal{D}[\sigma_z\otimes I]\rho \\ &+ \left(\gamma_{\varphi_{\mathbb{R}}} + \gamma_{{\rm dep}_{\mathbb{R}}}\right)\mathcal{D}[I\otimes\sigma_z]\rho \\ &+ \left(\gamma_{\varphi_{\mathbb{L}\mathbb{R}}} + \gamma_{{\rm dep}_{\mathbb{L}\mathbb{R}}}\right)\mathcal{D}[\sigma_z\otimes\sigma_z]\rho + \sum_{j<k}\gamma_{{\rm rel}_{jk}}\mathcal{D}[\sigma_{jk}]\rho,\end{aligned} \tag{5}$$

where $\gamma_{\varphi_{\mathbb{L}}}$ ($\gamma_{\varphi_{\mathbb{R}}}$) and $\gamma_{\varphi_{\mathbb{L}\mathbb{R}}}$ are the charge-noise dephasing rates for qubit $\mathbb{L}$ ($\mathbb{R}$) and the capacitive coupling α,

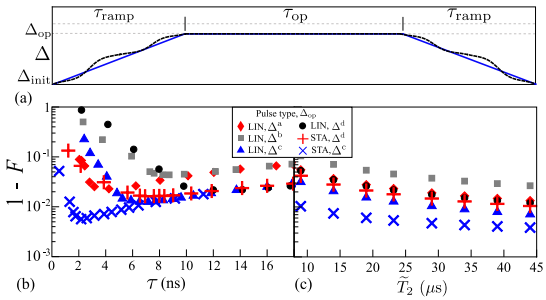

FIG. 4. (a) Detuning pulse sequences for the linear ramping scheme (LIN; solid line) and shortcut to adiabaticity (STA; dashed line). (b) CPHASE gate infidelities as a function of the total gate time τ for $\widetilde{T}_2 = 23$ μs. (c) CPHASE gate infidelities as a function of the reference charge-noise dephasing time $\widetilde{T}_2$ [53,54]. For each set of results, the gate time τ is chosen such that it produces the minimal gate infidelity as indicated in (b).

respectively. All of them are proportional to a reference charge-noise dephasing time, $\widetilde{T}_2 = 1/\widetilde{\gamma}_\varphi$ [53], which we shall use as our noise amplitude. $\gamma_{\rm rel}$ ($\gamma_{\rm dep}$) is the phonon-mediated relaxation (pure dephasing) rate. $\mathcal{D}[c]$ represents the dissipation superoperator $\mathcal{D}[c]\rho \equiv 2c\rho c^\dagger - c^\dagger c\rho/2 - \rho c^\dagger c/2$ [56]. More details, including the derivation of the decoherence rates listed above, can be found in Sec. IX of the Supplemental Material [53].

We have chosen $\Delta^{\rm a,b,c,d}$ as candidates of $\Delta_{\rm op}$ (as indicated in Fig. 2). The α values as well as $\partial J^{\rm eff}/\partial\Delta$ for these points are summarized in Table I. On the one hand, $\partial J^{\rm eff}/\partial\Delta$ is small for $\Delta^{\rm b,c,d}$, suggesting that the charge-noise-induced dephasing is suppressed. On the other hand, ramping the system to $\Delta^{\rm a,c}$ requires less detuning sweeps than $\Delta^{\rm b,d}$, suggesting that within the same $\tau_{\rm ramp}$, choosing $\Delta^{\rm a,c}$ as the operating points limits the leakage. These considerations imply that $\Delta^{\rm c}$ is the optimal choice for $\Delta_{\rm op}$.

We consider two ways of detuning the DDQD system from $\Delta_{\rm init}$ to $\Delta_{\rm op}$: a linear ramping scheme where $d\Delta/dt =$ const and one based on the shortcut to adiabaticity (STA) [see Fig. 4(a)] [57,58]. It is noticed that for $B = 0.104$ T, charge transitions of different logical states are either located at the same Δ (facilitated by the same interdot tunneling) or well separated in Δ values [see Fig. 2(d)], allowing us to apply concatenated STA pulse sequences, the details of which can be found in Sec. X of the Supplemental Material [53]. The application of STA pulse sequences allows the reduction of the total gate time τ without increasing the leakage, therefore suppressing decoherence. Note that the STA pulse sequence is not available for $\Delta^{\rm a,b}$ as the charge transitions occur very closely in Δ and cannot be individually addressed for different logical states [see Fig. 2(c)].

TABLE I. Summary of the parameters for different $\Delta_{\rm op}$.

B (T)	$\Delta_{\rm op}$	$\lvert\alpha\rvert$ (μeV)	$\partial J^{\rm eff}/\partial\Delta$
0	$\Delta^{\rm a}$	8.34	4.94×10^{-1}
	$\Delta^{\rm b}$	70.32	1.74×10^{-3}
0.104	$\Delta^{\rm c}$	57.2	7.50×10^{-3}
	$\Delta^{\rm d}$	7.52	2.83×10^{-3}

We numerically simulate the master equation, Eq. (5), taking into account the leakage by expanding $H_{\rm int}$ into the effective Hamiltonian block for each logical eigenstate [53]. The dephasing effect by hyperfine noise is neglected here as we found that the main limiting factors of the gate fidelity do not involve hyperfine fluctuation, for which the details are given in Sec. XII D in the Supplemental Material. The results of gate infidelities, $1 - F$ [59], as a function of τ and $\widetilde{T}_2$ are shown in Figs. 4(b) and 4(c), respectively. From Fig. 4(b), we see a reduction of infidelities at small τ for all results, but STA with operating point $\Delta^{\rm c}$ gives the lowest infidelity at the shortest gate operation time, while the linear scheme with $\Delta^{\rm c}$ gives the second-lowest infidelity. When τ is large, the infidelities increase with τ due to accumulated exposure to various decoherence channels other than leakage, as expected. Figure 4(c) shows the gate infidelities as a function of the reference charge-noise dephasing time $\widetilde{T}_2$, with the gate time τ for each set of results chosen such that it produces the minimal gate infidelity, as indicated in Fig. 4(b). We see that in the linear scheme, results calculated at $\Delta^{\rm c}$ exhibit about a factor of 2–4 reduction in infidelity compared to other $\Delta_{\rm op}$ values, while using the STA scheme offers another factor of 2–4. Therefore, the STA scheme in combination with the nearly sweet spot offers roughly an order of magnitude reduction in infidelities. We found out that similar results, including the existence of the nearly-sweet-spot region at large magnetic field and highest gate fidelity demonstrated by $\Delta^{\rm c}$, are achieved for a silicon DDQD device, the details of which are provided in Secs. V and XII in the Supplemental Material.

IV. CONCLUSIONS AND DISCUSSION

We have shown, using FCI calculations, that a range of nearly sweet spots, for both the single-qubit exchange energy and the capacitive coupling, appears in the coupled singlet-triplet qubit system under a strong enough external magnetic field. This range of nearly sweet spots arises due to the appearance of $|\widetilde{SS}\rangle$ and $|\widetilde{TT}\rangle$ states under magnetic field, which occupy detuning ranges that increase with the magnetic field.

It is interesting to compare our capacitive gates to exchange-mediated ones studied in the literature [44–50]. Our proposal should be easier to implement since it involves only detuning ramping, one degree of freedom less than exchange-mediated gates, which involve both the inter-DQD tunneling and detuning. On the other hand, for exchange gates, leakage into states with zero S_z is possible unless an additional magnetic field difference between the two DQDs is supplied. In contrast, capacitive gates are free from such leakage as the interdot tunneling is suppressed between two DQDs. Although leakage could occur when the detuning ramp passes through the charge transition points, it can be mitigated by pulse shaping or adiabatic ramping. In fact, we have demonstrated that ramping to and from the judiciously chosen nearly sweet spot using sequences based on the shortcut to adiabaticity offers maximal gate fidelities under charge noise and phonon-induced decoherence. Our results therefore should facilitate realization of high-fidelity two-qubit gates in coupled singlet-triplet qubit systems.

ACKNOWLEDGMENTS

G.X.C. and X.W. are supported by the Key-Area Research and Development Program of Guangdong Province (Grant No. 2018B030326001), the National Natural Science Foundation of China (Grant No. 11874312), the Research Grants Council of Hong Kong (Grants No. 11303617, No. 11304018, and No. 11304920), and the Guangdong Innovative and Entrepreneurial Research Team Program (Grant No. 2016ZT06D348). J.P.K. acknowledges support from the National Science Foundation under Grant No. 1915064 and the Army Research Office (ARO) under Grant No. W911NF-17-1-0287.

[1] J. R. Petta, A. C. Johnson, J. M. Taylor, E. A. Laird, A. Yacoby, M. D. Lukin, C. M. Marcus, M. P. Hanson, and A. C. Gossard, Science **309**, 2180 (2005).

[2] M. D. Shulman, O. E. Dial, S. P. Harvey, H. Bluhm, V. Umansky, and A. Yacoby, Science **336**, 202 (2012).

[3] J. Levy, Phys. Rev. Lett. **89**, 147902 (2002).

[4] X. Wu, D. R. Ward, J. R. Prance, D. Kim, J. K. Gamble, R. T. Mohr, Z. Shi, D. E. Savage, M. G. Lagally, M. Friesen, S. N. Coppersmith, and M. A. Eriksson, Proc. Natl. Acad. Sci. USA **111**, 11938 (2014).

[5] B. M. Maune, M. G. Borselli, B. Huang, T. D. Ladd, P. W. Deelman, K. S. Holabird, A. A. Kiselev, I. Alvarado-Rodriguez, R. S. Ross, A. E. Schmitz, M. Sokolich, C. A. Watson, M. F. Gyure, and A. T. Hunter, Nature (London) **481**, 344 (2012).

[6] C. Barthel, J. Medford, C. M. Marcus, M. P. Hanson, and A. C. Gossard, Phys. Rev. Lett. **105**, 266808 (2010).

[7] Z. Shi, C. B. Simmons, J. R. Prance, J. King Gamble, M. Friesen, D. E. Savage, M. G. Lagally, S. N. Coppersmith, and M. A. Eriksson, Appl. Phys. Lett. **99**, 233108 (2011).

[8] K. Takeda, A. Noiri, J. Yoneda, T. Nakajima, and S. Tarucha, Phys. Rev. Lett. **124**, 117701 (2020).

[9] P. Cerfontaine, T. Botzem, J. Ritzmann, S. S. Humpohl, A. Ludwig, D. Schuh, D. Bougeard, A. D. Wieck, and H. Bluhm, Nat. Commun. **11**, 4144 (2020).

[10] K. Eng, T. D. Ladd, A. Smith, M. G. Borselli, A. A. Kiselev, B. H. Fong, K. S. Holabird, T. M. Hazard, B. Huang, P. W. Deelman, I. Milosavljevic, A. E. Schmitz, R. S. Ross, M. F. Gyure, and A. T. Hunter, Sci. Adv. **1**, e1500214 (2015).

[11] A. Noiri, T. Nakajima, J. Yoneda, M. R. Delbecq, P. Stano, T. Otsuka, K. Takeda, S. Amaha, G. Allison, K. Kawasaki, Y. Kojima, A. Ludwig, A. D. Wieck, D. Loss, and S. Tarucha, Nat. Commun. **9**, 5066 (2018).

[12] P. Harvey-Collard, R. M. Jock, N. T. Jacobson, A. D. Baczewski, A. M. Mounce, M. J. Curry, D. R. Ward, J. M. Anderson, R. P. Manginell, J. R. Wendt, M. Rudolph, T. Pluym, M. P. Lilly, M. Pioro-Ladriére, and M. S. Carroll, in *2017 IEEE International Electron Devices Meeting (IEDM)* (IEEE, New York, 2017), pp. 36.5.1–36.5.4.

[13] G. Cao, H.-O. Li, T. Tu, L. Wang, C. Zhou, M. Xiao, G.-C. Guo, H.-W. Jiang, and G.-P. Guo, Nat. Commun. **4**, 1401 (2013).

[14] G. Shinkai, T. Hayashi, T. Ota, and T. Fujisawa, Phys. Rev. Lett. **103**, 056802 (2009).

[15] T. Hayashi, T. Fujisawa, H. D. Cheong, Y. H. Jeong, and Y. Hirayama, Phys. Rev. Lett. **91**, 226804 (2003).

[16] K. D. Petersson, J. R. Petta, H. Lu, and A. C. Gossard, Phys. Rev. Lett. **105**, 246804 (2010).

[17] Y. Dovzhenko, J. Stehlik, K. D. Petersson, J. R. Petta, H. Lu, and A. C. Gossard, Phys. Rev. B **84**, 161302(R) (2011).

[18] J. Gorman, D. G. Hasko, and D. A. Williams, Phys. Rev. Lett. **95**, 090502 (2005).

[19] Z. Shi, C. B. Simmons, D. R. Ward, J. R. Prance, R. T. Mohr, T. S. Koh, J. K. Gamble, X. Wu, D. E. Savage, M. G. Lagally, M. Friesen, S. N. Coppersmith, and M. A. Eriksson, Phys. Rev. B **88**, 075416 (2013).

[20] M. D. Reed, B. M. Maune, R. W. Andrews, M. G. Borselli, K. Eng, M. P. Jura, A. A. Kiselev, T. D. Ladd, S. T. Merkel, I. Milosavljevic, E. J. Pritchett, M. T. Rakher, R. S. Ross, A. E. Schmitz, A. Smith, J. A. Wright, M. F. Gyure, and A. T. Hunter, Phys. Rev. Lett. **116**, 110402 (2016).

[21] F. Martins, F. K. Malinowski, P. D. Nissen, E. Barnes, S. Fallahi, G. C. Gardner, M. J. Manfra, C. M. Marcus, and F. Kuemmeth, Phys. Rev. Lett. **116**, 116801 (2016).

[22] J. C. Abadillo-Uriel, M. A. Eriksson, S. N. Coppersmith, and M. Friesen, Nat. Commun. **10**, 5641 (2019).

[23] X.-C. Yang and X. Wang, Phys. Rev. A **96**, 012318 (2017).

[24] X.-C. Yang and X. Wang, Phys. Rev. A **97**, 012304 (2018).

[25] J. Medford, J. Beil, J. M. Taylor, E. I. Rashba, H. Lu, A. C. Gossard, and C. M. Marcus, Phys. Rev. Lett. **111**, 050501 (2013).

[26] J. M. Taylor, V. Srinivasa, and J. Medford, Phys. Rev. Lett. **111**, 050502 (2013).

[27] D. Kim, D. R. Ward, C. B. Simmons, J. K. Gamble, R. Blume-Kohout, E. Nielsen, D. E. Savage, M. G. Lagally, M. Friesen, S. N. Coppersmith, and M. A. Eriksson, Nat. Nanotechnol. **10**, 243 (2015).

[28] G. Cao, H.-O. Li, G.-D. Yu, B.-C. Wang, B.-B. Chen, X.-X. Song, M. Xiao, G.-C. Guo, H.-W. Jiang, X. Hu, and G.-P. Guo, Phys. Rev. Lett. **116**, 086801 (2016).

[29] Z. Shi, C. B. Simmons, D. R. Ward, J. R. Prance, X. Wu, T. S. Koh, J. K. Gamble, D. E. Savage, M. G. Lagally, M. Friesen, S. N. Coppersmith, and M. A. Eriksson, Nat. Commun. **5**, 3020 (2014).

[30] M. Russ and G. Burkard, J. Phys.: Condens. Matter **29**, 393001 (2017).

[31] F. K. Malinowski, F. Martins, P. D. Nissen, S. Fallahi, G. C. Gardner, M. J. Manfra, C. M. Marcus, and F. Kuemmeth, Phys. Rev. B **96**, 045443 (2017).

[32] Y.-P. Shim and C. Tahan, Phys. Rev. B **97**, 155402 (2018).

[33] J. M. Taylor, H. A. Engel, W. Dür, A. Yacoby, C. M. Marcus, P. Zoller, and M. D. Lukin, Nat. Phys. **1**, 177 (2005).

[34] J. M. Nichol, L. A. Orona, S. P. Harvey, S. Fallahi, G. C. Gardner, M. J. Manfra, and A. Yacoby, npj Quantum Inf. **3**, 3 (2017).

[35] E. Nielsen, R. P. Muller, and M. S. Carroll, Phys. Rev. B **85**, 035319 (2012).

[36] T. Hiltunen and A. Harju, Phys. Rev. B **90**, 125303 (2014).

[37] D. Buterakos, R. E. Throckmorton, and S. Das Sarma, Phys. Rev. B **100**, 075411 (2019).

[38] G. Ramon, Phys. Rev. B **84**, 155329 (2011).

[39] F. A. Calderon-Vargas and J. P. Kestner, Phys. Rev. B **91**, 035301 (2015).

[40] M. A. Wolfe, F. A. Calderon-Vargas, and J. P. Kestner, Phys. Rev. B **96**, 201307(R) (2017).

[41] D. Stepanenko and G. Burkard, Phys. Rev. B **75**, 085324 (2007).

[42] S. Yang and S. Das Sarma, Phys. Rev. B **84**, 121306(R) (2011).

[43] V. Srinivasa and J. M. Taylor, Phys. Rev. B **92**, 235301 (2015).

[44] R. Li, X. Hu, and J. Q. You, Phys. Rev. B **86**, 205306 (2012).

[45] J. Klinovaja, D. Stepanenko, B. I. Halperin, and D. Loss, Phys. Rev. B **86**, 085423 (2012).

[46] S. Mehl, H. Bluhm, and D. P. DiVincenzo, Phys. Rev. B **90**, 045404 (2014).

[47] M. P. Wardrop and A. C. Doherty, Phys. Rev. B **90**, 045418 (2014).

[48] D. Buterakos, R. E. Throckmorton, and S. Das Sarma, Phys. Rev. B **98**, 035406 (2018).

[49] D. Buterakos, R. E. Throckmorton, and S. Das Sarma, Phys. Rev. B **97**, 045431 (2018).

[50] P. Cerfontaine, R. Otten, M. A. Wolfe, P. Bethke, and H. Bluhm, Phys. Rev. B **101**, 155311 (2020).

[51] E. Nielsen, R. W. Young, R. P. Muller, and M. S. Carroll, Phys. Rev. B **82**, 075319 (2010).

[52] E. Barnes, J. P. Kestner, N. T. T. Nguyen, and S. Das Sarma, Phys. Rev. B **84**, 235309 (2011).

[53] See Supplemental Material at http://link.aps.org/supplemental/10.1103/PhysRevB.103.L161409 for more numerical results, theoretical analyses, and discussions, which includes Refs. [60–88].

[54] O. E. Dial, M. D. Shulman, S. P. Harvey, H. Bluhm, V. Umansky, and A. Yacoby, Phys. Rev. Lett. **110**, 146804 (2013).

[55] There are complications involving the $|T^{02}\rangle$ state, and all such notations in the main text should be understood as two electrons occupying the lowest two levels, i.e., $|T_{\mathrm{L}}^{02}\rangle$ in [53].

[56] H. M. Wiseman and G. J. Milburn, *Quantum Measurement and Control* (Cambridge University Press, Cambridge, 2009).

[57] X. Chen, A. Ruschhaupt, S. Schmidt, A. del Campo, D. Guéry-Odelin, and J. G. Muga, Phys. Rev. Lett. **104**, 063002 (2010).

[58] X. Chen, E. Torrontegui, and J. G. Muga, Phys. Rev. A **83**, 062116 (2011).

[59] The definition of gate fidelity F and the initial input state are explained in Sec. XI of [53].

[60] H. Bluhm, S. Foletti, D. Mahalu, V. Umansky, and A. Yacoby, Phys. Rev. Lett. **105**, 216803 (2010).

[61] M. A. Fogarty, K. W. Chan, B. Hensen, W. Huang, T. Tanttu, C. H. Yang, A. Laucht, M. Veldhorst, F. E. Hudson, K. M. Itoh, D. Culcer, T. D. Ladd, A. Morello, and A. S. Dzurak, Nat. Commun. **9**, 4370 (2018).

[62] D. M. Zajac, T. M. Hazard, X. Mi, K. Wang, and J. R. Petta, Appl. Phys. Lett. **106**, 223507 (2015).

[63] C. H. Yang, W. H. Lim, N. S. Lai, A. Rossi, A. Morello, and A. S. Dzurak, Phys. Rev. B **86**, 115319 (2012).

[64] L. P. Kouwenhoven, N. C. van der Vaart, A. T. Johnson, W. Kool, C. J. P. M. Harmans, J. G. Williamson, A. A. M. Staring, and C. T. Foxon, Z. Phys. **85**, 367 (1991).

[65] T. Gerster, A. Müller, L. Freise, D. Reifert, D. Maradan, P. Hinze, T. Weimann, H. Marx, K. Pierz, H. W. Schumacher, F. Hohls, and N. Ubbelohde, Metrologia **56**, 014002 (2018).

[66] S. W. Jung, T. Fujisawa, Y. Hirayama, and Y. H. Jeong, Appl. Phys. Lett. **85**, 768 (2004).

[67] L. Höglund, K. F. Karlsson, P. O. Holtz, H. Pettersson, M. E. Pistol, Q. Wang, S. Almqvist, C. Asplund, H. Malm, E. Petrini, and J. Y. Andersson, Phys. Rev. B **82**, 035314 (2010).

[68] B. P. Wuetz, M. P. Losert, A. Tosato, M. Lodari, P. L. Bavdaz, L. Stehouwer, P. Amin, J. S. Clarke, S. N. Coppersmith, A. Sammak, M. Veldhorst, M. Friesen, and G. Scappucci, Phys. Rev. Lett. **125**, 186801 (2020).

[69] K. Takashina, Y. Ono, A. Fujiwara, Y. Takahashi, and Y. Hirayama, Phys. Rev. Lett. **96**, 236801 (2006).

[70] S. Goswami, K. A. Slinker, M. Friesen, L. M. McGuire, J. L. Truitt, C. Tahan, L. J. Klein, J. O. Chu, P. M. Mooney, D. W. van der Weide, R. Joynt, S. N. Coppersmith, and M. A. Eriksson, Nat. Phys. **3**, 41 (2007).

[71] D. Culcer, L. Cywiński, Q. Li, X. Hu, and S. Das Sarma, Phys. Rev. B **82**, 155312 (2010).

[72] E. R. MacQuarrie, S. F. Neyens, J. P. Dodson, J. Corrigan, B. Thorgrimsson, N. Holman, M. Palma, L. F. Edge, M. Friesen, S. N. Coppersmith, and M. A. Eriksson, npj Quantum Inf. **6**, 81 (2020).

[73] V. Kornich, C. Kloeffel, and D. Loss, Phys. Rev. B **89**, 085410 (2014).

[74] C. G. Van de Walle, Phys. Rev. B **39**, 1871 (1989).

[75] M. Boissonneault, J. M. Gambetta, and A. Blais, Phys. Rev. A **79**, 013819 (2009).

[76] C. P. Scheller, S. Heizmann, K. Bedner, D. Giss, M. Meschke, D. M. Zumbühl, J. D. Zimmerman, and A. C. Gossard, Appl. Phys. Lett. **104**, 211106 (2014).

[77] D. Maradan, L. Casparis, T. M. Liu, D. E. F. Biesinger, C. P. Scheller, D. M. Zumbühl, J. D. Zimmerman, and A. C. Gossard, J. Low Temp. Phys. **175**, 784 (2014).

[78] R. M. Jock, N. T. Jacobson, P. Harvey-Collard, A. M. Mounce, V. Srinivasa, D. R. Ward, J. Anderson, R. Manginell, J. R. Wendt, M. Rudolph, T. Pluym, J. K. Gamble, A. D. Baczewski, W. M. Witzel, and M. S. Carroll, Nat. Commun. **9**, 1768 (2018).

[79] T. S. Koh, S. N. Coppersmith, and M. Friesen, Proc. Natl. Acad. Sci. USA **110**, 19695 (2013).

[80] K. Takeda, J. Kamioka, T. Otsuka, J. Yoneda, T. Nakajima, M. R. Delbecq, S. Amaha, G. Allison, T. Kodera, S. Oda, and S. Tarucha, Sci. Adv. **2**, e1600694 (2016).

[81] L. Petit, M. Russ, H. G. J. Eenink, W. I. L. Lawrie, J. S. Clarke, L. M. K. Vandersypen, and M. Veldhorst, arXiv:2007.09034.

[82] M. A. Nielsen, Phys. Lett. A **303**, 249 (2002).

[83] M. Horodecki, P. Horodecki, and R. Horodecki, Phys. Rev. A **60**, 1888 (1999).

[84] T. Ezaki, N. Mori, and C. Hamaguchi, Phys. Rev. B **56**, 6428 (1997).

[85] H.-O. Li, G. Cao, M. Xiao, J. You, D. Wei, T. Tu, G.-C. Guo, H.-W. Jiang, and G.-P. Guo, J. Appl. Phys. **116**, 174504 (2014).

[86] C. Bureau-Oxton, J. Camirand Lemyre, and M. Pioro-Ladrière, J. Visualized Exp. **81**, e50581 (2013).

[87] S. J. Angus, A. J. Ferguson, A. S. Dzurak, and R. G. Clark, Nano Lett. **7**, 2051 (2007).

[88] E. T. Henry, Ph.D. thesis, University of California, Berkeley, 2007.